Korean J. Chem. Eng., 39(10), 2783-2791 (2022)
DOI: 10.1007/s11814-022-1110-7

pISSN: 0256-1115
eISSN: 1975-7220

Experimental and computational phase behavior analysis of the PGME+CO_2 and PGMEA+CO_2 mixture at high pressures

Young-Taek Kwon*,‡, Duraisami Dhamodharan*,‡, Hwan Choi, Sung-Won Shim**, and Hun-Soo Byun*,†**

*Department of Chemical and Biomolecular Engineering, Chonnam National University, Yeosu, Jeonnam 59626, Korea
**Jaewon Industrial Co., Yeosu, Jeonnam 59618, Korea
(*Received 9 February 2022 • Revised 14 March 2022 • Accepted 15 March 2022*)

Abstract−The vapor+liquid equilibrium (VLE) for the 2-components of propylene glycol monomethyl ether (PGME) and propylene glycol monomethyl ether acetate (PGMEA) in high pressure (HP) supercritical carbon dioxide (*S-CO₂*) was evaluated. The solubility data determination was performed by the synthetic method at *T*=(313.2 to 393.2) K and *p*=(1.92 to 16.5) MPa. The obtained results indicated that the solubility of *S-CO₂* was found to increase monotonically with the increase of system temperature and mole fraction of PGME and PGMEA in binary (solute+solvent) mixtures. The solubility curve of PGME and PGMEA in the PGME+*S-CO₂* and PGMEA+*S-CO₂* models increases in connection with the increasing T at a steady pressure. The PGME+*S-CO₂* and PGMEA+*S-CO₂* models reveal *type-I* phase behavior (PB). The critical properties were achieved by Joback and Aspen plus method. Moreover, the experimental result adequately correlated with the Peng-Robinson equation of state (*P-R E-O-S*). Root mean square deviation (RMSD) for the PGME+*S-CO₂* [Joback: k_{ij}=0.0, h_{ij}=−0.060, Aspen: k_{ij}=0.0, h_{ij}=−0.065] and PGMEA+*S-CO₂* [Joback: k_{ij}=0.0, h_{ij}=0.0, Aspen: k_{ij}=0.0, h_{ij}=0.0] systems using two factors determined at 353.2 K was 9.07% (Joback), 10.98% (Aspen) and 4.03% (Joback), 4.78% (Aspen), respectively.

Keywords: Phase Behavior Measurement, PGME, PGMEA, Carbon Dioxide, *P-R* Equation of State

INTRODUCTION

Knowledge of binary mixtures of the P-type glycol ether containing supercritical fluids (*SCFs*) shows a significant role in chemical applications, chemical technology, and separation processes [1-4]. For these reasons, assessment of the phase equilibrium (bubble-point (BP), dew-point (DP), and critical-point (CP)) for solution components under *SCFs* is highly significant [5-11]. Carbon dioxide (CO_2) is commonly utilized as an environment-friendly *SCF* solvent due to its being low-cost, nontoxic, and nonflammable. Also, it is an effective solvent with nonpolar fragments. Thus, an understanding of the vapor+liquid equilibrium (VLE) of supercritical carbon dioxide (*S-CO₂*) and solute 2-component is demanded for fundamental purposes.

Phase behavior (PB) records for several 2-component (solute+carbon dioxide) models were stated by our group [12-15], McHugh et al. [16-18], and Cowie et al. [19-21]. We have described the at temperatures varying from 313.2 to 393.2 K and various distinct pressures [12-15]. Matsukawa and Otake [22] presented the at T from (313 to 373) K, pressures from (1.11 to 20.76) MPa and CO_2 molar fraction from (0.1 to 0.9). Sudhir et al. [23] measured the PB data for a binary system involving *S-CO₂* with imidazolium-based ionic liquids at the temperatures from (298 to 333) K, and at pressures ca. 15.0 MPa. Propylene glycol monomethyl ether (PGME) and propylene glycol monomethyl ether acetate (PGMEA) appear as a colorless liquid and show an effective solvent for epoxy, cellulose acetate butyrate, alkyd resins, nitrocellulose, acrylic, and phenolic. It exposes advantages in printing ink, cleaning applications, and variety of coating techniques. Especially, PGMEA is widely used as a semiconductor cleaner. Also, the phase equilibrium data are needed for high purity separation to waste PGMEA solution after use as a semiconductor cleaning agent.

To assist plant layout and separation of *S-CO₂*, it is important to know the phase behavior demonstrated by the solutes of interest with *S-CO₂* [24]. In the active monomer units, glycol ethers are a vital commercial monomer along with a considerable broad variety of industrial applications. Most glycol ether systems are used as an intermediate in the manufacture of printing ink, cleaning applications, and variety of coating techniques. Because of this, it is necessary to explore the thermodynamic behavior of these varieties of monomer units. In most cases, for certain connections among polymer molecules and solvent such as hydrogen attachment, it is vital to be mindful that the connections amid particles can be changed by modifying the operating medium (*p* and *T*) in the support of the promising connections amid polymer units and mixture solvent. The dynamic support to the solubility is likely to be reliant on the solution molar density (or volume) and the mutual energy of combining amongst polymer units and solvent [25,26]. Nevertheless, the PB performance for the polymer-solvent (two component) system has been stated by several scientists. The laboratory investigations have been consistently brought out by Byun's team [27,28], McHugh's team [29,30], Radosz's team [31,32], and Kiran's team [33].

Herein, we investigated the PB of solution systems with super-

†To whom correspondence should be addressed.
E-mail: hsbyun@jnu.ac.kr
‡First and second authors contributed equally.

critical region of carbon dioxide in PGME and PGMEA monomers. The PGME+*S*-CO_2 and PGMEA+*S*-CO_2 mixtures at high pressure are reported at pressure up to 16.5 MPa and several temperatures (313.2-393.2 K). Improving an analytical thermodynamic model to precisely compute the thermodynamic behavior, PB of pure components is essential for various processes. For adjusting this thermodynamic model, the experimental results are modeled using the Peng-Robinson equation of state (*P-R E-O-S*) for the vapor and liquid phases. Though, there are many *E-O-S* systems available, the *P-R E-O-S* system is approached widely owing to its easiness, high accuracy in signifying the interactions between temperature and pressure, and phase structure in multi-component systems. The *P-R E-O-S* simulated results of proposed binary model (PGME+*S*-CO_2 and PGMEA+*S*-CO_2) exhibit a good agreement with the lab-made investigational data.

MATERIAL AND METHODS

1. Chemicals

PGME (mass fraction purity: >0.995, CAS RN 107-98-2, $C_4H_{10}O_2$) and PGMEA (mass fraction purity: >0.995, CAS RN 108-65-6, $C_6H_{12}O_3$) employed in this research was purchased from Sigma-Aldrich Co. All the materials were utilized as received in this study. CO_2 (mass fraction purity: >0.999) is acquired from Daehan Gases Co. was used as obtained. The stipulations of all the materials performed in this research are concise in Table 1 and the chemical molecular structural arrangement of PGME and PGMEA is represented in Fig. 1.

2. Apparatus and Procedure

The high-pressure (HP) phase behavior was studied by utilizing HP equipment, which is depicted in detail elsewhere [12-15]. The pictorial representation of the device is displayed in Fig. 2. The device primarily comprises three sections: HP generator, variable volume view (3V) cell, and display system. The HP generator (HIP, model 37-5.75-60) is operated to manage a piston (2.54 cm) by utilizing water and assessed with a Heise gauge (Dresser Ind., model CM-53920, 0-34.00 MPa) uncertainty to ±0.02 MPa. The dew-point (DP), mixture critical point, and bubble-point (BP) were obtained employing the 3V cell comprising a volume of ~28 cm^3, outer dia of 6.4 cm and inner dia of 1.59 cm, operating at a highest-pressure value about 70 MPa. To check the different phase transformation of the reaction mixture, a sapphire window about 1.9 cm dia×1.9 cm thickness was placed in the head of the part cell. A video display was employed to cross-check the inner cell reaction mixture, which is attached to a borescope camera (Olympus Corp, model F100-038-000-50).

Initially, the nitrogen gas was introduced into the 3V cell to remove traces of unwanted air and organic matters. Then, an HP bomb was utilized to inject *S*-CO_2 into the reaction cell within the uncertainty of ±0.002 g. The reaction mixture in the cell was flattened and retained in a mono phase by handling a piston at the

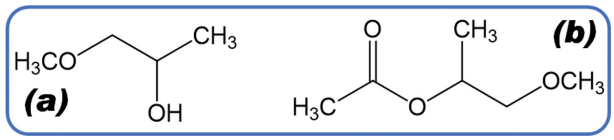

Fig. 1. Schematics structure of propylene glycol monomethyl ether (a) and propylene glycol monomethyl ether acetate (b) used in this work.

Table 1. Specifications of the chemicals used in this work

Chemical name	Mass fraction purity	Source	CAS RN
CO_2	>0.999	Daehan Gases Co.	124-38-9
Propylene glycol monomethyl ether	>0.995	Sigma-Aldrich Co.	107-98-2
Propylene glycol monomethyl ether acetate	>0.995	Sigma-Aldrich Co.	108-65-6

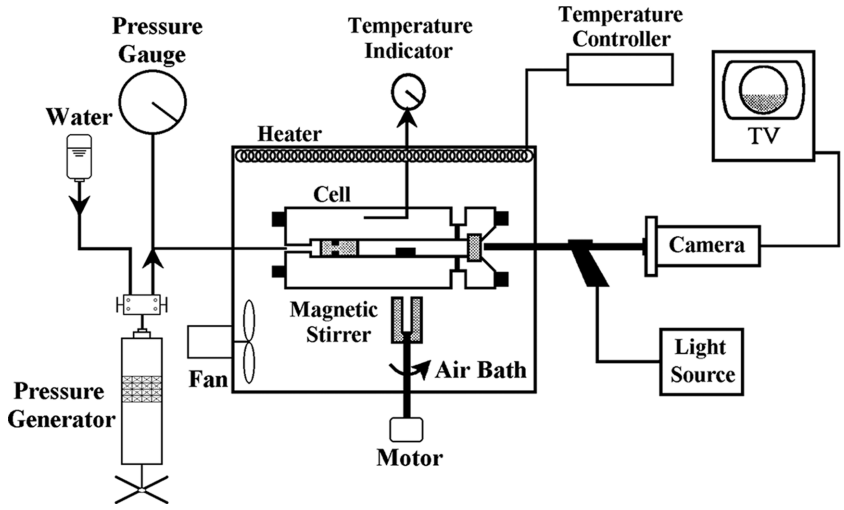

Fig. 2. Schematic diagram of high-pressure apparatus as shown in Ref. [12].

Table 2. The properties of pure components of carbon dioxide, propylene glycol monomethyl ether and propylene glycol monomethyl ether acetate

Compounds	M_w	Chemical structure	T_b/K	T_c/K	p_c/MPa	ω
Carbon dioxide	44.01	O=C=O		304.2	7.38	0.225
Propylene glycol monomethyl ether	90.12	$CH_3CH(OH)CH_2OCH_3$	391.2-392.2[a]	554.4[b]	4.44[b]	0.705[b]
				553.0[c]	4.34[c]	0.722[c]
Propylene glycol monomethyl ether acetate	130.16	$CH_3CO_2CH(CH_3)CH_2OCH_3$	419.2[d]	597.8[b]	3.09[b]	0.493[b]
				597.9[c]	3.01[c]	0.481[c]

[a]Sigma-Aldrich, [b]Joback method, [c]Aspen plus method, [d]Wikipedia

required pressure. To achieve a phase equilibrium in the reaction cell, the monophase of the reaction mixture was maintained for about 30-40 minutes at the preferred temperature. Then, the pressure was gently lowered till the different phase turned up. When a tiny vapor bubble was noticeable in the 3V cell, we stated it as a bubble point, while formation of the small fog in the 3V cell was described as a dew point. The critical point was stated when iridescence was noted together with equal vapor and liquid volume upon the development of the another phase as we altered the operating pressure and temperature in the mixture [34]. To attain more data, system temperature was modified and then the entire operating process was recurring. In this study a theoretical investigation was conducted using P-R [35] equations of state with van der Waals rule using two interaction parameters.

3. Modeling by Peng-Robinson (*P-R*) *E-O-S*

The *P-R E-O-S* [35] is expressed as given below:

$$P = \frac{RT}{v-b} - \frac{a(T)}{v(v+b)+b(v-b)} \quad (1)$$

$$a(T) = 0.45724\frac{R^2T_c^2}{P_c}\alpha(T_r, \omega) \quad (2)$$

$$b(T_c) = 0.07780\frac{RT_c}{P_c} \quad (3)$$

$$\alpha(T_r, \omega) = (1+\kappa(1-T_r^{1/2}))^2 \quad (4)$$

where, κ is defined as,

$$\kappa = 0.37464 + 1.5422\omega - 0.26999 \quad (5)$$

The rules are given below:

$$a_{mix} = \Sigma_i\Sigma_i x_i x_j a_{ij} \quad (6)$$

$$b_{mix} = \Sigma_i\Sigma_i x_i x_j b_{ij} \quad (7)$$

$$a_{ij} = (a_{ii}a_{jj})^{1/2}(1-\kappa_{ij}) \quad (8)$$

$$b_{ij} = \frac{1}{2}(b_{ii}+b_{jj})(1-\eta_{ij}) \quad (9)$$

where, κ_{ij} and η_{ij} are two component dealing factors and are obtained by lessening the following objective function:

$$OF = \Sigma_i^N\left(\frac{P_{exp}-P_{cal}}{P_{exp}}\right)^2 \quad (10)$$

$$RMSD\ (\%) = \sqrt{\frac{OF}{N}}100 \quad (11)$$

where, N is the number of laboratory investigational data. The subscripts "exp" and "cal" denote laboratory investigational and calculated bubble points. We performed with the least square approach employing "PYTHON" programming (scipy.optimize.least_squares) to lessen the objective function (OF). Table 2 displays the neat constituent acentric factors (ω), critical pressures (p_c), and critical temperatures (T_c) for carbon dioxide, PGMEA and PGME, which were calculated by using *P-R* equation. We utilized the prevailing boiling points from the literature [36]. The thermodynamics characters of PGMEA and PGME were determined by the Joback-Lyderson approach [34]. Additionally, the vapor pressures were attained by the Aspen approach [34].

RESULTS AND ANALYSIS

High-pressure PB records for the PGME and PGMEA in *S-CO_2* were evaluated, and the lab-made investigational uncertainty was anticipated to be 0.05 MPa and 0.2 K for a given loading of the cell [14,15] and the typical uncertainty for the mole fraction of PGME and PGMEA was 0.002 [15].

Fig. 3 represents the lab-made pressure-composition (*p-x*) isotherms at *T*=(313.2, 333.2, 353.2, 373.2 and 393.2) K, and pressures from (1.92 to 16.45) MPa for the (PGMEA+*S-CO_2*) model.

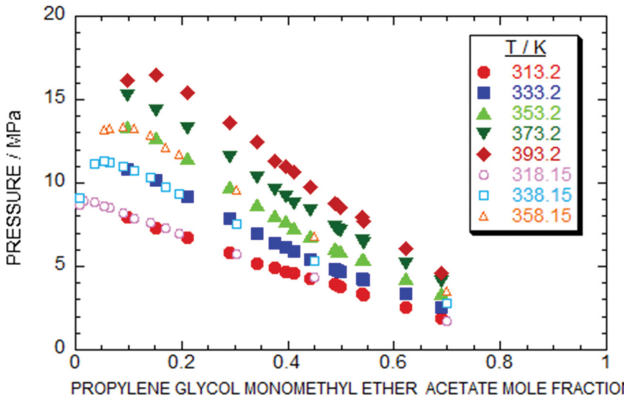

Fig. 3. Represent the lab-made pressure-composition (*p-x*) isotherms at *T*=(313.2, 333.2, 353.2, 373.2 and 393.2) K, and pressures from (1.92 to 16.45) MPa for the (PGMEA+*S-CO_2*) model. To verify the consistency of the laboratory equipment, the PB data for a 2-component (PGMEA+*S-CO_2*) mixture with the mole fractions as a mixture assessed earlier by Lee group [2006] at 318.15, 338.15 and 358.15 K.

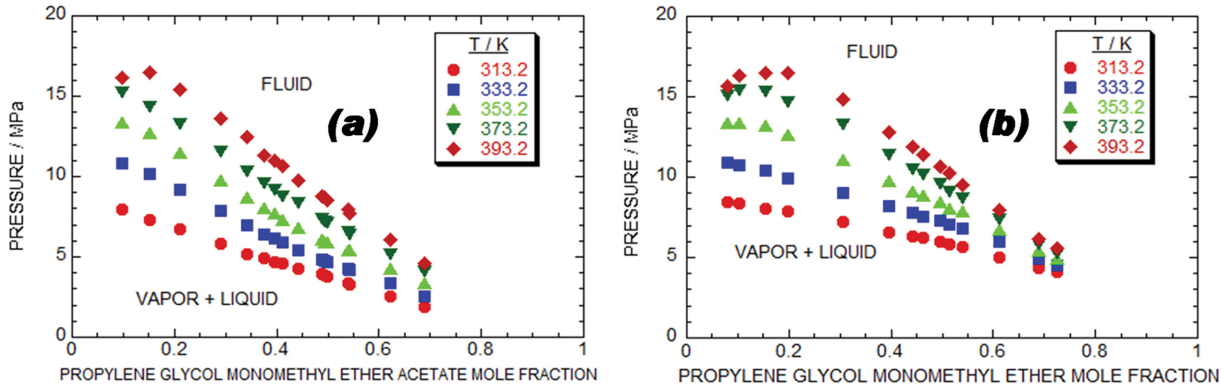

Fig. 4. Laboratory investigated pressure composition isotherm for (a) (1−*x*) PGMEA+*x S-CO*$_2$, and (b) (1−*x*) PGME+*x S-CO*$_2$ systems at various temperatures of 313.2 K, 333.2 K, 353.2 K, 373.2 K, and 393.2 K.

First, to verify the consistency of the laboratory equipment, we assessed the PB data for a 2-component (PGMEA+*S-CO*$_2$) mixture with the mole fractions as a mixture assessed earlier by the Lee group [2006] at 318.15, 338.15 and 358.15 K [26]. As demonstrated in Fig. 3, the laboratory records were in good fit with prevailing consistent data. Herein, three phases were not detected at any of the five operated T, and the *p-x* isotherms (see Fig. 3) are reliable with those anticipated for the *type-I* system [27]. Then, the solubility rose with respect to the rising temperatures at the mole fraction of PGMEA.

Fig. 4(a) and Table 3 expose the lab-made results (*p-x*) isotherms at T of 313.2-393.2 K and at pressures starting from 1.92-16.45 MPa for the (1-*x*) PGMEA+*x S-CO*$_2$ model. Fig. 4(b) and Table 4 display the lab-made results at temperatures of 313.2-393.2 K and at pressures starting from 4.33-16.52 MPa for the (1−*x*) PGME+*x S-CO*$_2$ model. According to Fig. 4(a) and (b), the *p-x* isotherms are exhibiting the *type-I* system and there were no three phases observed at any of the five operated temperatures. Besides, the solubility of the carbon dioxide was noted as reducing with the respect to the increasing temperature at steady pressure.

Fig. 5 symbolizes the pressures versus mole fraction comparative study of the lab-made data (symbols) with simulated results (solid lines) achieved from Joback method (a) and Aspen method (b) performed by *P-R E-O-S* for the ((1−*x*) PMGE+*x S-CO*$_2$) system at 353.2 K. As displayed in Fig. 5, the computed curves were achieved employing the optimized values established at each T. In extent of this study, RMSD (%) value of bubble point pressure analyzed utilizing fitted dealings factors for the as-proposed two component model ((1−*x*) PMGE+*x S-CO*$_2$) utilizing *P-R E-O-S* at temperature 353.2 K is 2.64% (Joback approach) and 4.73% (Aspen method). Here, data point is 13 at each operated temperature. The optimized factor values for the (1-*x*) PGME+*x S-CO*$_2$ system by Joback and Aspen methods were κ_{ij}=0.0 and η_{ij}=−0.060 (refer Fig. 5(a)) and κ_{ij}=0.0 and η_{ij}=−0.065 (refer Fig. 5(b)). As demonstrated in Fig. 5(a) and (b), PB for the ((1−*x*) PMGE+*x S-CO*$_2$) system showed good agreement in the comparison between the lab-made records and simulated curves.

Fig. 6(a) and (b) shows the comparative study between lab-made record and simulated values by critical properties obtained from Joback method (a) and Aspen method (b) performed by *P-R E-O-S* for the ((1−*x*) PMGEA+*x S-CO*$_2$) system. As shown in Table 2, the critical properties reported from Aspen method [26] and obtained Joback group contribution by boiling point [24]. Fig. 6(a) shows the comparison results between the lab-made results and simulated values by critical properties (p_c, T_c and ω) obtained from Joback method. The simulated values of altered binary interaction

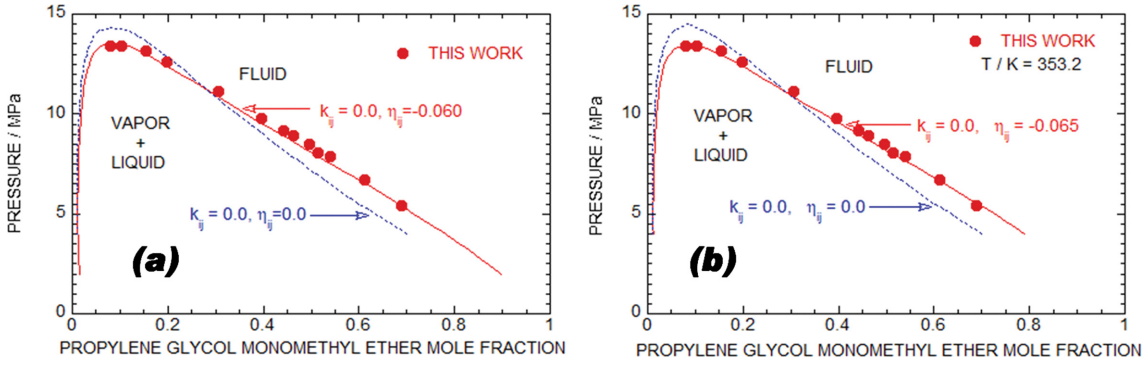

Fig. 5. Symbolizes the pressures verses mole fraction comparative study of the lab-made data (symbols) with simulated results (solid lines) achieved from Joback method (a) and Aspen method (b) performed by *P-R E-O-S* for the ((1−*x*) PMGE+*x S-CO*$_2$) system at 353.2 K. The circles indicate to laboratory experimental data points, solid line shows fit of *P-R E-O-S*. Dotted blue lines signify results with k$_{ij}$=0.0, η_{ij}=0.0 whereas red colored lines signify results with fitted k$_{ij}$ and η_{ij}.

Table 3. Experimental data for the propylene glycol monomethyl ether acetate (PGMEA)+*S-CO₂* system in this work. BP is a Bubble-Point, CP is a Critical-Point and DP is a Dew-Point

PGMEA mole fraction	p[a]/MPa	Transition[b]	PGMEA mole fraction	p[a]/MPa	Transition[b]
	T/K=313.2			T/K=333.2	
0.099	7.93	BP	0.099	10.83	BP
0.151	7.33	BP	0.151	10.21	BP
0.210	6.70	BP	0.210	9.21	BP
0.290	5.79	BP	0.290	7.84	BP
0.341	5.19	BP	0.341	6.97	BP
0.376	4.92	BP	0.376	6.39	BP
0.395	4.71	BP	0.395	6.11	BP
0.411	4.58	BP	0.411	5.94	BP
0.442	4.30	BP	0.442	5.42	BP
0.488	3.93	BP	0.488	4.85	BP
0.492	3.87	BP	0.492	4.76	BP
0.499	3.80	BP	0.499	4.68	BP
0.540	3.37	BP	0.540	4.26	BP
0.543	3.30	BP	0.543	4.22	BP
0.621	2.51	BP	0.621	3.38	BP
0.689	1.92	BP	0.689	2.59	BP
	T/K=353.2			T/K=373.2	
0.099	13.38	BP	0.099	15.28	BP
0.151	12.72	BP	0.151	14.34	BP
0.210	11.48	BP	0.210	13.29	BP
0.290	9.76	BP	0.290	11.55	BP
0.341	8.69	BP	0.341	10.37	BP
0.376	8.04	BP	0.376	9.63	BP
0.395	7.68	BP	0.395	9.23	BP
0.411	7.31	BP	0.411	8.79	BP
0.442	6.81	BP	0.442	8.33	BP
0.488	6.10	BP	0.488	7.39	BP
0.492	5.94	BP	0.492	7.26	BP
0.499	5.88	BP	0.499	7.16	BP
0.540	5.42	BP	0.540	6.54	BP
0.543	5.38	BP	0.543	6.43	BP
0.621	4.29	BP	0.621	5.20	BP
0.689	3.39	BP	0.689	4.09	BP
	T/K=393.2				
0.099	16.17	DP			
0.151	16.45	CP			
0.210	15.39	BP			
0.290	13.64	BP			
0.341	12.45	BP			
0.376	11.33	BP			
0.395	10.97	BP			
0.411	10.66	BP			
0.442	9.75	BP			
0.488	8.82	BP			
0.492	8.71	BP			
0.499	8.57	BP			
0.540	7.93	BP			
0.543	7.72	BP			
0.621	6.07	BP			
0.689	4.59	BP			

[a]Standard uncertainties u are u(T)=0.3 K, u(p)=0.05 MPa and u(x)=0.003

[b]BP is a Bubble-Point, CP is a Critical-Point and DP is a Dew-Point

Table 4. Experimental data for the propylene glycol monomethyl ether (PGME)+*S-CO*$_2$ system in this work. BP is a Bubble-Point, CP is a Critical-Point and DP is a Dew-Point

PGME mole fraction	p[a]/MPa	Transition[b]	PGME mole fraction	p[a]/MPa	Transition[b]
	T/K=313.2			T/K=333.2	
0.081	8.47	BP	0.081	10.90	DP
0.104	8.35	BP	0.104	10.75	DP
0.153	8.07	BP	0.153	10.39	DP
0.197	7.85	BP	0.197	9.90	CP
0.257	7.62	BP	0.257	9.53	BP
0.306	7.21	BP	0.306	9.01	BP
0.360	6.98	BP	0.360	8.56	BP
0.397	6.59	BP	0.397	8.17	BP
0.443	6.31	BP	0.443	7.80	BP
0.462	6.21	BP	0.462	7.58	BP
0.497	5.98	BP	0.497	7.27	BP
0.513	5.86	BP	0.513	7.09	BP
0.541	5.66	BP	0.541	6.80	BP
0.613	4.97	BP	0.613	5.97	BP
0.690	4.33	BP	0.690	4.90	BP
	T/K=353.2			T/K=373.2	
0.081	13.39	DP	0.081	15.07	DP
0.104	13.39	DP	0.104	15.38	DP
0.153	13.19	DP	0.153	15.31	DP
0.197	12.62	DP	0.197	14.70	DP
0.257	12.11	CP	0.257	14.22	DP
0.306	11.11	BP	0.306	13.28	CP
0.360	10.46	BP	0.360	12.29	BP
0.397	9.79	BP	0.397	11.40	BP
0.443	9.15	BP	0.443	10.49	BP
0.462	8.89	BP	0.462	10.16	BP
0.497	8.49	BP	0.497	9.62	BP
0.513	8.06	BP	0.513	9.09	BP
0.541	7.86	BP	0.541	8.69	BP
0.613	6.72	BP	0.613	7.38	BP
0.690	5.40	BP	0.690	5.84	BP
	T/K=393.2				
0.081	15.66	DP			
0.104	16.31	DP			
0.153	16.48	DP			
0.197	16.52	DP			
0.257	15.91	CP			
0.306	14.84	BP			
0.360	14.08	BP			
0.397	12.82	BP			
0.443	11.90	BP			
0.462	11.37	BP			
0.497	10.67	BP			
0.513	10.29	BP			
0.541	9.55	BP			
0.613	7.97	BP			
0.690	6.18	BP			

[a]Standard uncertainties u are u(T)=0.3 K, u(p)=0.05 MPa and u(x)=0.003

[b]BP is a Bubble-Point, CP is a Critical-Point and DP is a Dew-Point

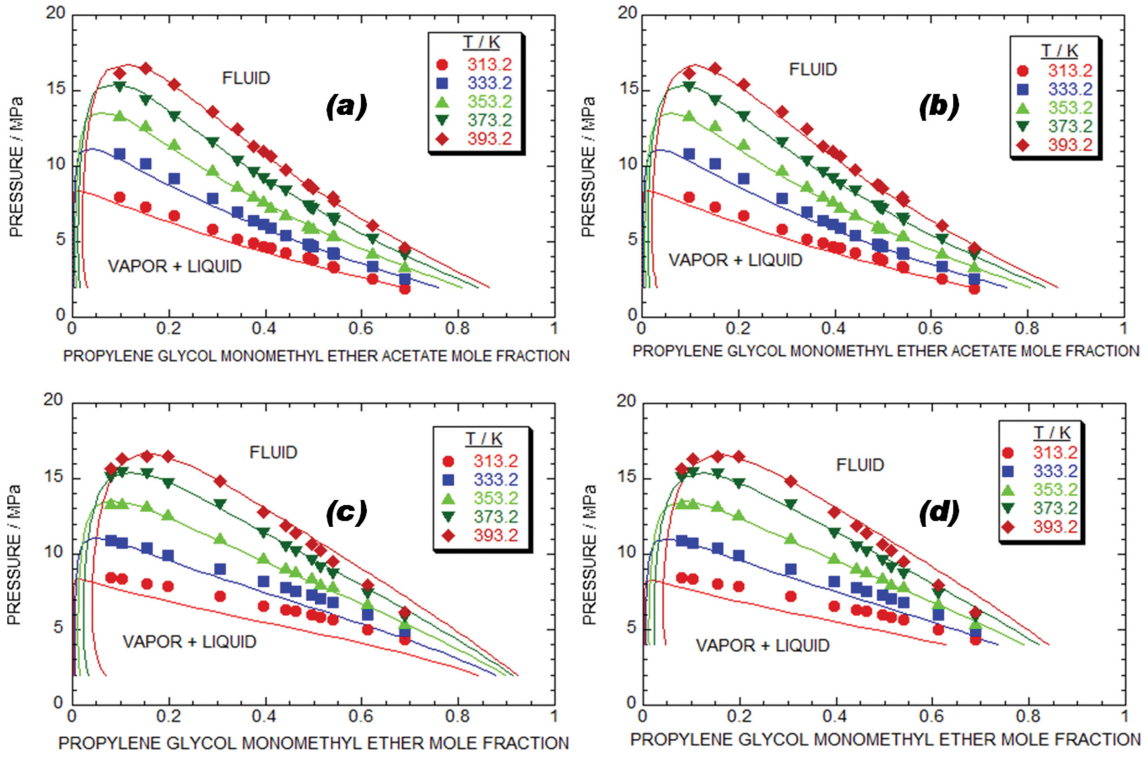

Fig. 6. Shows the comparative study between lab-made record and simulated values by critical properties obtained from Joback method (a) and Aspen method (b) performed by *P-R E-O-S* for the (1−*x*) PGMEA+*x Sc-CO₂* system at various temperatures of 313.2 K, 333.2 K, 353.2 K, 373.2 K, and 393.2 K. The comparative study between lab-made record and simulated values by critical properties obtained from Joback method (c) and Aspen method (d) performed by *P-R E-O-S* for the (1−*x*) PGME+*x S-CO₂* system at various temperatures of 313.2 K, 333.2 K, 353.2 K, 373.2 K, and 393.2 K.

factors (κ_{ij} and η_{ij}) obtained employing the *P-R* equation at 353.2 K were matched with the lab-made investigational data. The optimized factor values for the (1−*x*) PGMEA+*x S-CO₂* system was κ_{ij}=0.0 and η_{ij}=0.0 (data points: 14; RMSD: 1.61%). RMSD (%) for the ((1−*x*) PGMEA+*x S-CO₂*) system at several temperatures applying the factors calculated at 353.2 K were 4.03% (data points: 70). The comparison results of calculated and experimental curves were observed as a good agreement by two interaction factors: κ_{ij}=η_{ij}=0.0.

Fig. 6(b) demonstrates the comparison between the lab-made records with simulated (*p-x*) isotherms at (313.2-393.2) K for the ((1−*x*) PGMEA+*x S-CO₂*) model employing the optimized κ_{ij} and η_{ij} values calculated at 353.2 K. The critical properties (T_c=597.9 K, p_c=3.01 MPa) of necessarily using the *P-R* equation was obtained by literature (Aspen method). RMSD (%) for the altered factor (κ_{ij}=0.0 and η_{ij}=0.0) values for the ((1−*x*) PGMEA+*x S-CO₂*) system at 353.2 K was 2.68% (data points: 14). RMSD (%) for the ((1−*x*) PGMEA+*x S-CO₂*) model at the 5 temperatures employing the factors calculated (κ_{ij}=0.0 and η_{ij}=0.0) were 4.78% (data points: 70).

Fig. 6(c) shows the comparison study of lab-made records with simulated data by critical properties (p_c, T_c and ω) achieved from Joback approach. The simulated records of altered binary interaction factors (κ_{ij} and η_{ij}) achieved by employing the *P-R* equation at 353.2 K were fitted with the lab-made data. The optimized factor values for the PGME+*S-CO₂* system were κ_{ij}=0.0 and η_{ij}=0.0. RMSD for the ((1−*x*) PGME+*x S-CO₂*) system at serval temperatures utilizing the factors calculated at 353.2 K was 9.07% (data points: 65). The comparison results of calculated and experimental curves were observed as a good agreement by two interaction factors: κ_{ij}=η_{ij}=0.0.

Fig. 6(d) demonstrates the comparison between the lab-made records with simulated (*p-x*) isotherms at (313.2-393.2) K for the ((1−*x*) PGME+*x S-CO₂*) model applying the optimized κ_{ij} and η_{ij} values calculated at 353.2 K. The critical properties (T_c=553.0 K, p_c=4.34 MPa) of necessarily using the *P-R* equation were obtained by literature (Aspen method). The optimized factor values for the (1−*x*) PGME+*x S-CO₂* system was κ_{ij}=0.0 and η_{ij}=0.0. RMSD (%) for the ((1−*x*) PGME+*x S-CO₂*) model at the five temperatures utilizing the factors calculated (κ_{ij}=0.0 and η_{ij}=0.0) were 10.98% (data points: 65).

Fig. 7(a) (Joback Method) and (b) (Aspen Method) show the mixture-critical curves (MCP) between lab-made records and simulated data by the *P-R* equation for the (PGMEA+*S-CO₂*) model using altered interaction factors (κ_{ij}=0.0 and η_{ij}=0.0) at 353.2 K. The simulated MCP is *type-I*. Red solid lines correspond to the vapor pressure of pure CO_2 and PGMEA determined by Joback (a) and Aspen (b) methods. The blue solid circles indicate the CP of pure CO_2 and PGMEA. The top of the blue line represents 1-phase, the bottom area indicates 2-phases. The blue solid lines correspond to the computed values achieved from the *P-R E-O-S*, with κ_{ij}=0.0 and η_{ij}=0.0 (PGMEA+*S-CO₂*) ((a) and (b)). The blue solid squares are the MCP ascertained from isotherms in experi-

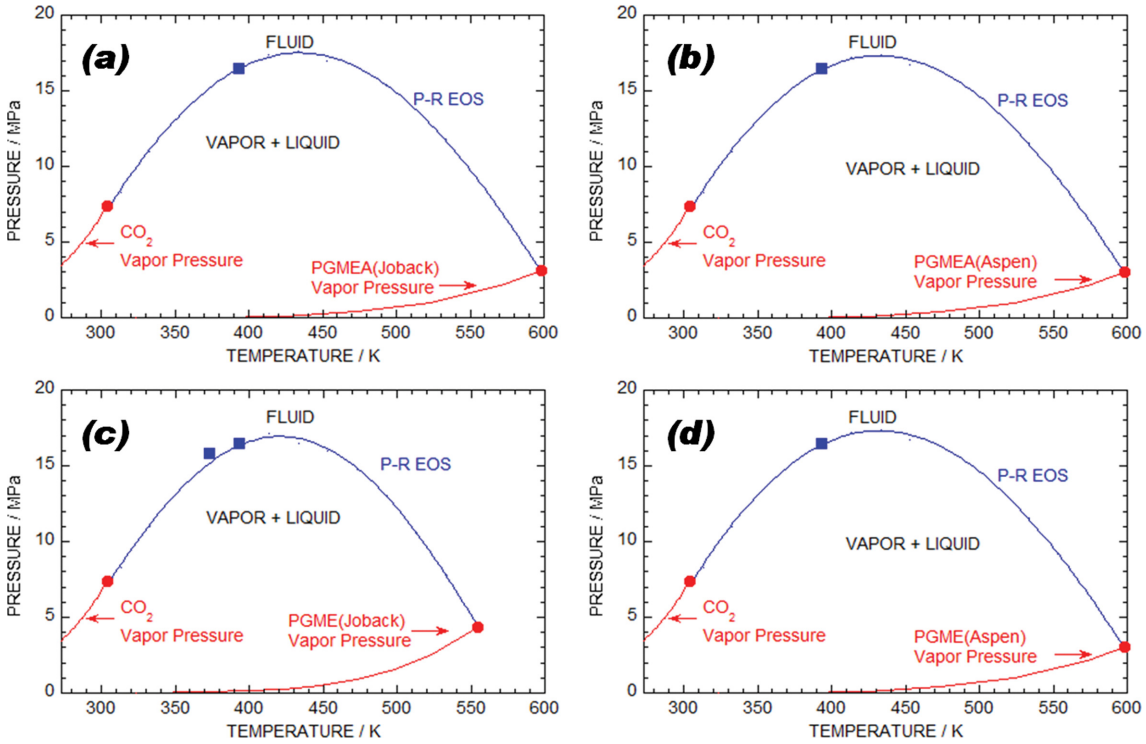

Fig. 7. (a) (Joback Method) and (b) (Aspen Method) show the mixture-critical curves (MCP) between lab-made records and simulated data by the *P-R* equation for the (PGMEA+*S*-CO_2) model using altered interaction factors (κ_{ij}=0.0 and η_{ij}=0.0) at 353.2 K. Red solid lines correspond to the vapor pressure of pure CO_2 and PGMEA determined by Joback (a) and Aspen (b) method. The blue solid circles indicate the CP of pure CO_2 and PGMEA. (c) (Joback Method) and (d) (Aspen Method) show the mixture-critical curves (MCP) between lab-made records and simulated data by the *P-R* equation for the (PGME+*S*-CO_2) model using altered interaction factors (κ_{ij}=−0.065, η_{ij}=−0.095 by Joback (c) and κ_{ij}=0.0, η_{ij}=−0.065 by Aspen (d)) at 353.2 K. Red solid lines correspond to the vapor pressure of pure CO_2 and PGME determined by Joback (c) and Aspen (d) approach. The blue solid circles denote the CP of pure CO_2 and PGME. Solid squares are critical points determined from isotherms measured in this work.

mentation measured.

Fig. 7(c) (Joback Method) and (d) (Aspen Method) show the mixture-critical curves (MCP) between lab-made records and simulated data by the *P-R* equation for the PGME+*S*-CO_2) model using altered interaction factors (κ_{ij}=−0.065, η_{ij}=−0.095 by Joback (c) and κ_{ij}=0.0, η_{ij}=−0.065 by Aspen (d)) at 353.2 K. The simulated MCP is *type-I*. Red solid lines correspond to the vapor pressure of pure CO_2 and PGME determined by Joback (c) and Aspen (d) approach. The blue solid circles denote the CP of pure CO_2 and PGME. The top of the blue line represents 1-phase, the lower region indicates 2-phase. The blue solid squares are the MCP ascertained from isotherms in experimentation measured.

CONCLUSIONS

New lab-made investigational data for the (PGME+*S*-CO_2) and (PGMEA+*S*-CO_2) binary systems at high and low pressure was studied by synthetic apparatus using the direct visual inspection method at T varying from (313.2 to 393.2) K and pressure up to ~16.5 MPa. The (PGME+*S*-CO_2) and (PGMEA+*S*-CO_2) mixture did not show three phases (liquid+liquid+vapor) at the five operated temperatures. The *P-R E-O-S* moderately predicted the phase behavior for the (PGME+*S*-CO_2) and (PGMEA+*S*-CO_2) models employing two temperature-independent component interaction factors. The MCP among the simulated and lab-made investigational records are reasonably in a good fit when contemplating two alterable factors of the *P-R E-O-S* used. RMSD (%) for the PGME+*S*-CO_2 [Joback: κ_{ij}=0.0, η_{ij}=−0.060, Aspen: κ_{ij}=0.0, η_{ij}=−0.065] and CO_2+PGMEA [Joback: κ_{ij}=0.0, η_{ij}=0.0, Aspen: κ_{ij}=0.0, η_{ij}=0.0] systems employing two factors calculated at 353.2 K were 9.07% (Joback method), 10.98% (Aspen method) and 4.03% (Joback method), 4.78% (Aspen method), respectively.

ACKNOWLEDGEMENTS

This research was supported by Ministry of Trade, Industry & Energy (MOTIE), Korea Institute for Advancement of Technology (KIAT) through "A supporting program for the middle market enterprises in each region" (No. P0017536).

NOMENCLATURE

Symbols

a : fascination factor [Pa·m^6/mol^2]
b : Co-volume factor [m^3/mol]
BP : bubble point [MPa]
CP : critical point
DP : dew point

N : number of the data points
P : pressure [Pa]
R : universal gas constant [8.314462 J/(mol·K)]
T temperature [K]
v : molar volume [$m^3 \cdot mol^{-1}$]
x : liquid phase mole fractions

Greek Letters

α : alpha function
ω : acentric factor

Abbreviations

E-O-S : equation of state
OF : objective function
P-R : Peng-Robinson

REFERENCES

1. K. Zelijko, D. Cor and M. K. Hrncic, *J. Chem. Eng. Data*, **63**, 860 (2018).
2. G. J. Philip and L. Walter, *Chemical synthesis using supercritical fluids*, Weinheim, Wiley-VCH (1999).
3. G. Brunner, *Annu. Rev. Chem. Biomol. Eng.*, **1**, 321 (2010).
4. L.-S. Anne, C. Aymonier and F. Cansell, *J. Chem. Technol. Biot.*, **85**, 583 (2010).
5. H.-S. Byun and H.-Y. Lee, *J. Chem. Eng. Data*, **51**, 1436 (2006).
6. H.-S. Byun, M.-Y. Choi and J.-S. Lim, *J. Supercrit. Fluids*, **37**, 323 (2006).
7. Y.-S. Jang, H.-H. Jeong and H.-S. Byun, *J. Ind. Eng. Chem.*, **18**, 414 (2012).
8. S.-H. Kim, M.-H. Park, J.-S. Lim and H.-S. Byun, *J. Ind. Eng. Chem.*, **16**, 962 (2010).
9. S.-H. Cho, D.-S. Yang and H.-S. Byun, *Fluid Phase Equilib.*, **351**, 18 (2013).
10. C.-R. Kim and H.-S. Byun, *Fluid Phase Equilib.*, **381**, 51 (2014).
11. S.-H. Cho, C.-R. Kim, S.-D. Yoon and H.-S. Byun, *Fluid Phase Equilib.*, **396**, 74 (2015).
12. H.-S Byun and D.-H. Lee, *Ind. Eng. Chem. Res.*, **45**, 3354 (2006).
13. H.-S Byun, B. M. Hasch and M. A. McHugh, *Fluid Phase Equilib.*, **115**, 179 (1996).
14. H.-S. Byun and C. Park, *Korean J. Chem. Eng.*, **19**, 126 (2002).
15. H.-S. Byun and J.-S. Shin, *J. Chem. Eng. Data*, **48**, 97 (2003).
16. L. Michele and M. A. McHugh, *Fluid Phase Equilib.*, **157**, 285 (1999).
17. Y. Wu, M. S. Newkirk, S. T. Dudek, K. Williams, V. Krukonis and M. A. McHugh, *Ind. Eng. Chem. Res.*, **53**, 10133 (2014).
18. J. Liu, D. Li, H.-S. Byun and M. A. McHugh, *Fluid Phase Equilibria*, **267**, 39 (2008).
19. J. M. G. Cowie and I. J. McEwen, *Polymer*, **24**, 1453 (1983).
20. J. M. G. Cowie and I. J. McEwen, *J. Chem. Soc., Faraday Trans. 1: Phys. Chem. Condensed Phases*, **70**, 171 (1974).
21. J. M. G. Cowie and I. J. McEwen, *British Polymer J.*, **7**, 459 (1975).
22. H. Matsukawa, A. Fujii, T.-A. Hoshina and K. Otake, *J. Chem. Eng. Data*, **548**, 113172 (2021).
23. N. V. K. A. Sudhir, B. R. Mellein, E. M. Saurer and J. F. Brennecke, *J. Phys. Chem. B*, **108**, 20355 (2004).
24. M. A. McHugh and V. J. Krukonis, *Supercritical fluid extraction*, 2nd ed., Butterworth-Heinemann, Stoneham (1994).
25. M. A. McHugh, F. Rindfleisch, P. T. Kuntz, C. Schmaltz and M. Buback, *Polymer*, **39**, 6049 (1998).
26. S.-H. Lee, M. A. LoStracco, B. M. Hasch and M. A. McHugh, *J. Phys. Chem.*, **98**, 4055 (1994).
27. P. N. P. Ghoderao, D. Dhamodharan and H.-S. Byun, *J. Chem. Thermodyn.*, **168**, 106746 (2022).
28. S.-H. Cho, C.-R. Kim, S.-D. Yoon and H.-S. Byun, *Fluid Phase Equilib.*, **396**, 74 (2015).
29. R. R. Mallepally, V. S. Gadepalli, B. A. Bamgbade, N. Cain and M. A. McHugh, *J. Chem. Eng. Data*, **61**, 2818 (2016).
30. Y. Wu, M. S. Newkirk, S. T. Dudek, K. Williams, V. Krukonis and M. A. McHugh, *Ind. Eng. Chem. Res.*, **53**, 10133 (2014).
31. K. L. Albrecht, F. P. Stein, S. J. Han, C. J. Gregg and M. Radosz, *Fluid Phase Equilib.*, **117**, 84 (1996).
32. B. Folie, C. Gregg, G. Luft and M. Radosz, *Fluid Phase Equilib.*, **120**, 11 (1996).
33. E. Kiran, *J. Supercrit. Fluids*, **110**, 126 (2016).
34. B. E. Poling, J. M. Prausnitz and J. P. O'connell, *The properties of gases and liquids*, Vol. 5, McGraw-Hill, New York (2001).
35. D. Y. Peng and D. B. Robinson, *Ind. Eng. Chem. Fundam.*, **15**, 59 (1976).
36. C.-T. Hsieh, M.-J. Lee and H.-M. Lin, *Ind. Eng. Chem. Res.*, **45**, 2123 (2006).
37. L. S. Robert and P. H. van Konynenburg, *Discuss. Faraday Soc.*, **49**, 87 (1970).